

Solid Propellant Rocket Motor Insensitive Munitions, Testing and Simulation

Dr. A. Weigand*, G. Unterhuber*,
K. Kupzik**, Dr. T. Eich***, B. Bucher***

Abstract: The present paper summarizes the major results of the German Technology Program on the IM behaviour of solid-propellant rocket motors. The program extended over a period of four years (from 2006 to 2009) and was contracted by the German DoD and WTD91, Meppen, to Co. Bayern-Chemie, a subsidiary of MBDA-Germany. A total of 15 tactical size rocket motors were tested using Carbon Fibre Composite (CFC) motor cases in combination with two composite solid propellants. The propellants consisted of 80% Ammoniumperchlorate (AP) and 20 % HTPB-binder and featured two different burn-rates: 20 mm/s and 40 mm/s at 100 bar pressure and 20°C soak-temperature conditions. All rocket motor tests were conducted at the WTD91 proving ground in Meppen and included the IM-aggressions Bullet Attack (BA), Fast Heating (FH) and Slow Heating (SH). The tests were conducted according to AOP-39 and the related STANAG's. Where applicable additional sensors recorded motor head-end pressure, axial thrust and external as well as internal motor- and propellant-temperatures. Due to the high effort in testing and the resulting severity in terms of STANAG reaction type, numerical modelling focused on the SH case. Using small-scale DSC tests in order to obtain data of the propellant reaction kinetics, the simulation of the SH case resulted in accurate predictions of the reaction time. Together with high-temperature burn-rate measurements, the SH prediction capability led to a successful mitigation of the reaction type by early-ignition.

1. Introduction

Insensitive Munitions (IM) has evolved into one of the most important current research and development topics in tactical missile and, in particular, in solid propellant rocket motor design. The IM Technology Study reported here was funded by the German DoD and extended over a period of four years. The major goals of that study were:

1. Create a knowledge- and data-base on the IM behaviour of solid propellant rocket motors, which translated to: "Improve and design new rocket-motor specific IM test set-ups and technologies at the WTD91 proving ground and study the motor behaviour under different IM aggressions".
2. Develop computer models that are able to predict the IM behaviour of solid propellant rocket motors in order to minimize the number of large-scale tests and to reduce motor development costs.
3. Improve the IM characteristics of solid propellant rocket motors by studying the effects of motor design, propellant formulation, burn rate and mitigation.

Section 2 gives an overview on the investigated motor designs. In Sec. 3, the results of the conducted IM tests Bullet Attack (BA), Fast Heating (FH) and Slow Heating (SH), the latter with and without mitigation, are reported. Section 4 discusses the results of SH-simulations and Sec. 5 concludes with a summary and outlook.

Presented at the 2010 Insensitive Munitions & Energetic Materials Technology Symposium, 11-14 October, 2010, Munich, Germany.

* Bayern-Chemie GmbH, MBDA Germany, Liebigstr. 17, 84544 Aschau, Germany

** Wehrtechn. Dienststelle f. Waffen u. Munition, WTD91-330, Schießplatz, 49716 Meppen, Germany

*** Wehrtechn. Dienststelle f. Waffen u. Munition, WTD91-320, Schießplatz, 49716 Meppen, Germany

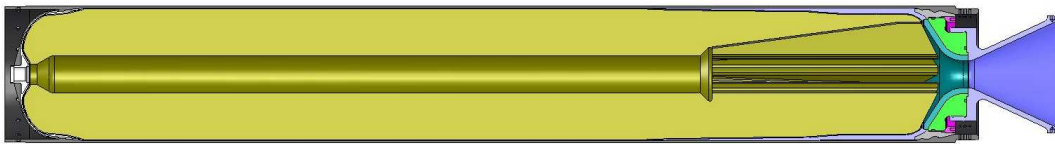
2. Motor Description

Figure 1 shows sectional views of the two types of rocket motors that were tested within the IM Technology Program. As the data in Table 1 indicate, both motor types feature the same Carbon Fibre Composite (CFC) case with a calibre of 168 mm, a length of 1180 mm, and an internal thermal insulation made out of EPDM (rubber). The nozzles are thermally equivalent dummy nozzles with insulated entrance sections. The expansion cones are made out of steel and are not insulated. In the tests, the IM motors were not equipped with igniters.

The CFC-cases were filled with two different burn-rate composite propellants (basic formulation: 80% Ammoniumperchlorate and 20% HTPB-binder). The first motor type was filled with a comparatively low burn-rate (LBR) propellant with a burn rate of 20 mm/s at standard conditions of 20°C soak temperature and 100 bar pressure. The second motor type exhibits a high burn-rate (HBR) propellant with a standard condition burn-rate of 40 mm/s.

The LBR motor has a fin-o-cyl grain with a web fraction of 70% and a propellant mass of 32 kg. In order to remain within the operative pressure limits of the CFC-case, the throat diameter of the HBR motor had to be enlarged by a factor of two in accordance to the burn-rate and initial burn-surface ratio. Therefore, a double cylindrical grain with a relatively large bore diameter was chosen here to make sure that the throat (i.e., the critical flow condition, $Ma = 1$) is located in the nozzle and not anywhere in the bore. The web fraction of the HBR grain is therefore only 50% with a propellant mass of 24 kg. Both types of grains are case-bonded to the EPDM insulation via a thin layer of liner material.

- „low“ burn-rate propellant (20 mm/s at 100bar, +20°C) , mTZ = 32 kg:



- „high“ burn-rate propellant (>40 mm/s at 100bar, +20°C), mTZ = 24 kg:

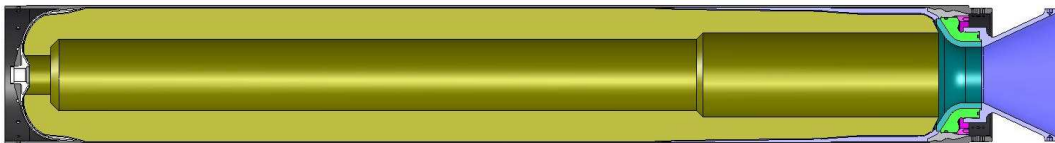


Figure 1: Sectional views of the two IM rocket motors.

Properties	Motor 1 (low burn rate, LBR)	Motor 2 (high burn rate, HBR)
case	CFC	CFC
internal thermal insulation	EPDM	EPDM
propellant	composite	composite
grain shape (case bonded)	fin-o-cyl	double cylindrical
calibre, mm	168	168
length, mm	1180	1180
throat diameter, mm	33	66
burn rate, mm/s @ Tsoak=20°C, p=100bar	20	40
web fraction, %	70	50
propellant mass, kg	32	24

Table 1: IM rocket-motor characteristics.

3. IM Testing

3.1 Overview

As part of the IM Technology Program, 15 rocket motors using 7 low burn-rate (LBR) and 8 high burn-rate (HBR) motors were tested at the WTD91 proving ground in Meppen.

Table 2 gives an overview on the tested IM aggressions with the number and type of tested motors. Also, the measurement and test equipment are listed. Please note, that all tests were conducted in close agreement with AOP-39, ed.2 and the specific test STANAG's, ed.2. However, as already stated in the introduction, the goal of the IM Technology Program was not to perform a particular reaction-type classification (IM-map) of a rocket motor, but to improve existing and define new test set-ups/technologies at the proving ground and to study (no to qualify) the motor behaviour under different IM aggressions. Therefore, in some cases, for example during Fast Heating tests, deviating STANAG wind conditions were accepted.

Due to the danger of Kerosin spilling and the possible environmental damage to the soil, FH-Kerosin fires are not allowed at WTD91 in combination with explosive materials. Therefore, as Table 2 indicates, Propane gas fires were used instead, except in two cases, where a wood fire was used mostly out of historical reasons and reasons of comparison. Numerous measurement techniques were applied on the range and on the rocket motor itself in order to study the IM behaviour of the motors. Table 2 gives an overview on the applied measurement techniques which typically included thermocouples (T), strain gauges (D), pressure (P) and thrust (S) sensors on motor level, and infrared cameras (IR), hi-speed video (HV), video (V), blast pressure (BL) and bullet speed (BS) sensors on the test range.

IM-Aggression	Number of tests	LBR Motor	HBR Motor	P	S	T	B L	V	H V	IR	D	B S
Bullet Attack (BA)	4	1	3	x	x	-	x	x	x	-	x	x
Fast Heating, wood fire (FH-wood)	2	1	1	x	x	x	x	x	-	-	-	-
Fast Heating, gas fire (FH-gas)	4	3	1	x	x	x	x	x	-	x	-	-
Slow Heating (SH)	5	2	3	x	-	x	x	x	-	-	-	-
Total	15	7	8									

Table 2: IM rocket-motor tests, test- and measurement equipment.

3.2 Bullet Attack Tests (BA)

As Table 2 shows, 4 Bullet Attack tests (STANAG 4241) were conducted with 1 LBR and 3 HBR motors. The 0,5 inch M2 AP (AP-Armour Piercing) bullets were measured to reach penetration speeds in the range of 810 m/s to 830 m/s which is just at the lower end of the required speed of 850 ± 20 m/s. The measured exit speeds resulted to be in the range of 700 m/s to 750 m/s.

As Fig. 2 shows, the target was located in the center of the rocket motor and had a diameter of 50 mm. Independent of the burn rate, the penetration of the bullet ignited all tested motors by the friction between bullet and propellant grain. In terms of failure mechanism, Figure 3 indicates that the CFC-cases were only damaged locally, i.e., in a region of 1 to 2 calibres surrounding the penetration point of the bullet. That local damage was found to be typical for all conducted BA tests and is caused by the exiting and simultaneously tumbling bullet. The latter destroys the hoop layers of the CFC-case and damages the structural integrity of the "pressure vessel". Therefore, the recorded pressure and thrust data, shown in Fig. 4, indicate only short duration (< 5 ms) initial pressure and thrust peaks in the range of the nominal motor pressure and thrust level. A significant pressure and thrust built-up during the motor burn was not observed.



Figure 2: Bullet Attack test set-up, IM-motor on thrust-measurement test stand.



Figure 3: Bullet Attack test, case damage.

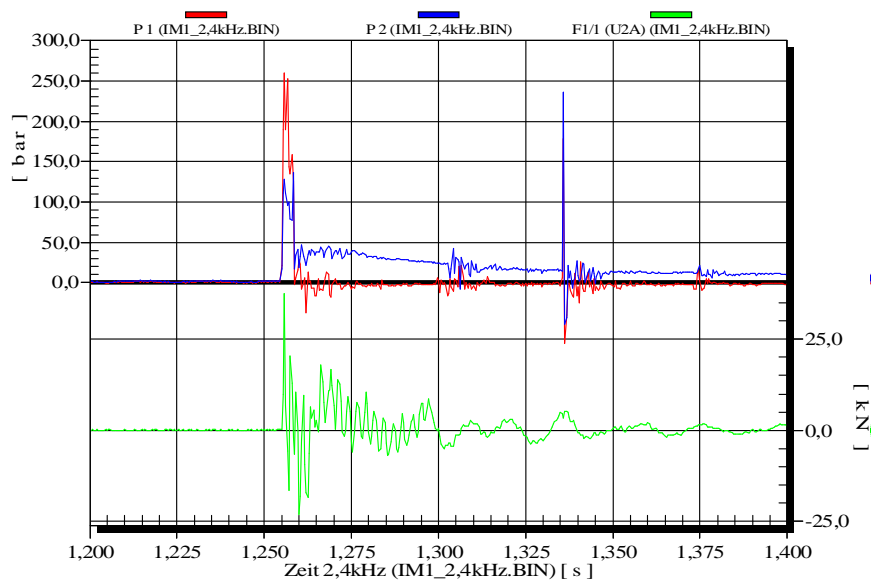


Figure 4: Bullet Attack test, results of pressure and thrust measurements.

The results of blast pressure measurements in 5 m distance to the motor center revealed that the threshold of 45 mbar was not exceeded in any of the conducted tests. Also, most of the debris such as un-burned pieces of propellant and small carbon fibre bundles were found within a radius of 15 m and along the bullet trajectory between gun and motor and motor downwards.

In addition to the single-bullet firings, a triple salvo was fired in one test which, however, did not change the ignition behaviour and the case damage significantly. This indicates that the second and third bullet penetrate into the already damaged region of the motor having only a minor or even no effect on the overall reaction behaviour.

3.3 Fast Heating Tests (FH)

A total of 6 Fast Heating tests using twice wood- and 4 times gas-fires were performed. Here, the results of gas-fire tests (STANAG 4240) with 3 LBR and 1 HBR motor are reported.

Figure 5 shows the gas-fire test stand at WTD91 with the rocket motor being secured by a cage - satisfying safety regulations of the range. The motor is free to move axially such that axial thrust can be measured using a thrust balance that is located outside of the gas fire.



Figure 5: Fast Heating gas-fire test stand with motor thrust-balance set-up.

All FH motors were equipped with a series of thermocouples fixed to the outside of the motor-case. Figure 6a shows the STANAG conform results of the fire temperature measurements which indicate that the gas fire reaches the 550°C temperature threshold well before the 30s limit, and that the average fire temperatures remain well above the required 800°C level during the entire test (the drop of fire temperature M15 to 700°C during the last 7s of the test might have been caused by some local up-draft or wind; it is not regarded to be critical in the context here). In contrast to that, Fig. 6b shows the evolution of case temperatures along the circumference of the motor. The data indicate local temperature differences of up to 200K. Those differences are not only caused by the local flame and flow field (as is the case at M01 which is located in the flow-separation region downstream of the cylindrical case), but also result from the motor location and the distribution of the gas burners. In that regard, the study revealed that the wind protection and the gas-burner set up must be improved for a better and more homogeneous temperature distribution in the fire.

Nevertheless, the FH gas-fire tests showed that the reaction time of the 4 tested rocket motors was in a relatively narrow range of 60 s to 84 s (measured from the time, when at least 2 of 4 fire temperatures reached the threshold of 550°C). A possible explanation for this is the fact that the motor reaction time is predominantly driven by the heat flux (fire property), the heat transfer/conduction to/of the case, and the ignition temperature of the case-bonded

propellant. The case/EPDM-insulation compound is the same in both motor types and the ignition temperatures of the two composite propellants are also similar under FH conditions. Therefore, the motor reaction time remained in a relatively narrow range which, on the other hand, speaks for the repeatability of the gas-fire conditions.

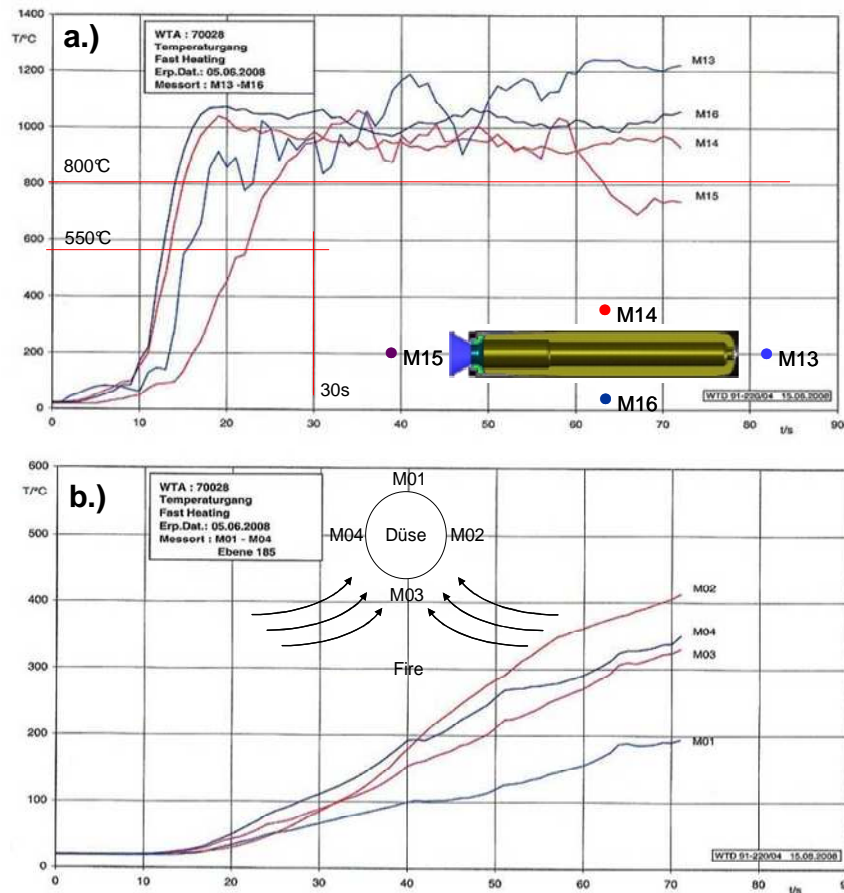


Figure 6a,b: Fast Heating (a) fire- and (b) motor-surface temperatures

Two different reaction types were observed during the FH tests:

1.) The **Local & Slow Reaction** is characterized by the weakening of the CFC-case due to the heat of the fire (i.e., pyrolysis of the epoxy resin) and an almost atmospheric burn of the motor that evolves in two stages. Stage 1: The case bonded grain is locally ignited at the bondline and burns a hole into the case from inside out. Simultaneously, the grain burns inside towards the bore under atmospheric pressure conditions, i.e., with a very slow burn rate. The radial burn causes a cone in the grain and a side jet that blows off through the hole increasing the hole size even further. Stage 2: Once the flame front reaches the bore of the grain, the bore-surface ignites, and the residual grain burns off through the already formed hole in the side of the case – again, under near atmospheric pressure and, hence, slow-burn conditions. This relatively controlled burn with formation of a side jet leads to a mild FH reaction without strong pressure/thrust built-up, nor any case/motor fragmentation.

2.) The **Global & Fast Reaction** is characterized by the simultaneous ignition of a comparatively large part of the bonding-area. This leads to a sudden pressure built-up and a subsequent failure of the thermally weakened case structure. Fragments of the CFC case and pieces of the propellant grain are spread (half) spherically and isotropically over an area with radius $\gg 15$ m. The reaction also causes blast pressures of up to 250 mbar in 5m distance from the nozzle exit and, therefore, leads to a reaction type that is more severe than in the case of the Local & Slow Reaction described above. One can speculate that the simultaneous failure of a large part of the bonding area might be the result of thermal out-gassing processes of the EPDM-insulation and/or the liner material at high temperatures.

3.4 Slow Heating Tests (SH)

As Table 2 shows, 5 Slow Heating tests (STANAG 4382) with were conducted with 2 LBR and 3 HBR motors. One of the 3 HBR SH-motors was equipped with an igniter which was used to initiate the motor and mitigate the SH reaction (see Sec. 3.5).

Due to WTD91 safety regulations, the SH tests had to be conducted in an open bunker, or, similar to the FH tests, with the motor being placed in a protective cage. Figure 7 shows the SH test set-up with cage. In contrast to the bunker tests, this set up allowed for the installation of blast pressure sensors.

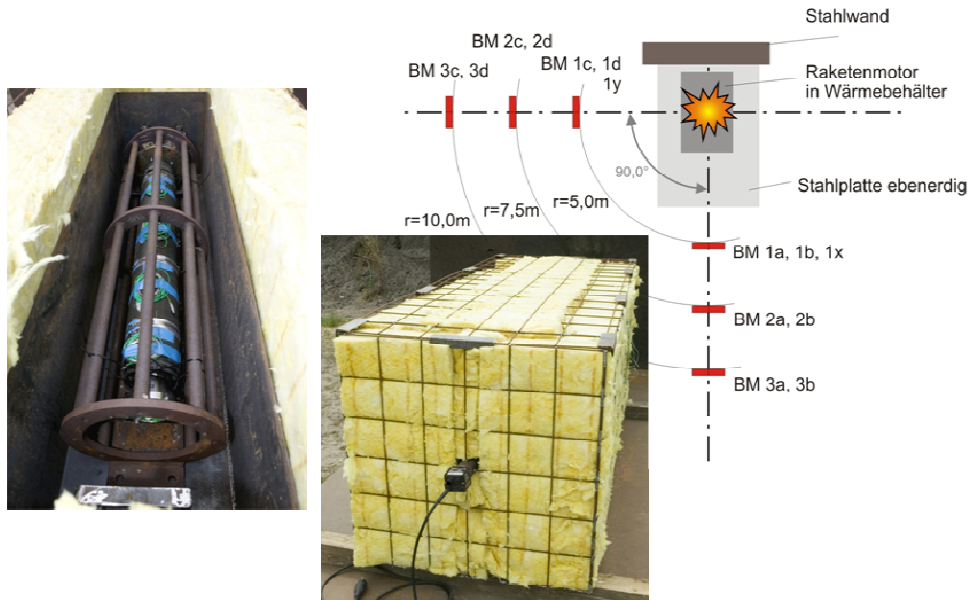


Figure 7: Slow Heating test set-up, oven, cage and location of blast-pressure sensors.

The oven is operated by a temperature controller and 2 air-blower/heater sets (one on each face of the oven). The controller adjusts the 3.3°C oven-temperature gradient by switching the 4 kW power output of the air heaters. As Fig. 7 shows, the blast meters are located in the axial (BM1a,1b...) and lateral (BM1c,1d...) direction of the motor at a distance of 5 m, 7.5 m and 10 m. All blast meters were centered at the height of motor axis level.

Figure 8 shows the evolution of the oven- and motor-temperatures of a SH test with a HBR motor. Motor temperatures were measured in the bore (gas volume) and along the motor surface. The four required oven temperatures (STANAG 4382) are well within a temperature range of $\pm 3^\circ\text{C}$, while the motor surface -temperatures indicate a small spatial temperature difference in the oven of less than 6 K.

The data in Fig. 8 show that subsequent to a 12h/50°C constant-temperature soak phase, the HBR motor reacted after 34.5 h at an oven temperature of 162°C. The reaction of the motor was severe with maximum blast pressures of 4.6 bar, 2 bar and 1 bar in 5 m, 7.5 m and 10 m distance, respectively. The blast pressure data also agree well with the observation of severe reaction levels during the aforementioned SH bunker-tests.

The repeatability of the reaction temperatures and reaction times (which are, off course, coupled via the 3.3°C oven-temperature gradient) was found to be excellent. The reaction temperatures and times of the 2 LBR motors were in both tests 195°C and 43.1h, while those of the 2 HBR motors resulted to be at a much lower level of 162°C and 34,5h and 164°C and 34,8h. The difference of the LBR and HBR reaction temperatures amounts to 32 K which is equivalent to a heating period of almost 10h! This behaviour was also observed in small-scale DSC calorimetry tests in which the temperature threshold of exothermal reactions of the HBR propellant was found to be much lower than that of the LBR propellant. The latter is caused by the different burn-rate modifiers that were used in the propellant formulations.

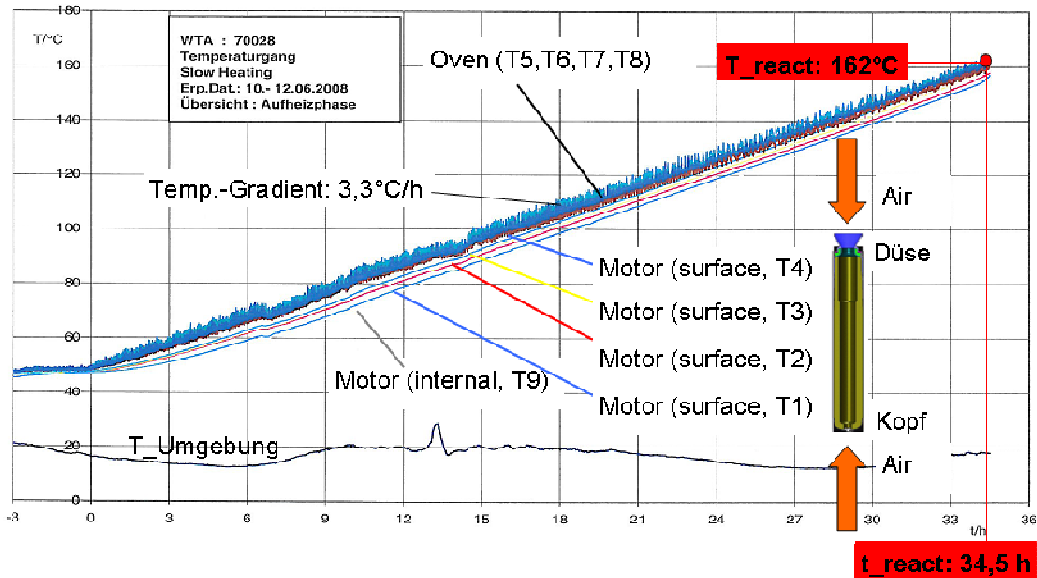


Figure 8: Evolution of oven- and motor-temperatures during a HBR SH-test.

Briefly summarized, one can state that the SH reaction temperatures (and also the reaction times) do strongly depend on the propellant formulation and the applied burn-rate modifiers. However, independent of the two investigated composite propellants, the resulting SH reaction levels were in both cases severe.

3.5 Slow Heating Mitigation

As mentioned in the beginning of Sec. 3.4, one SH test used an HBR motor with an integrated igniter. The purpose of that test was to clarify the following important questions:

- 1.) Can an igniter be qualified at soak temperature levels much greater than the typical upper soak-temperature limits of, let's say, +71°C?
- 2.) Does the motor, once ignited at such high soak-temperatures, burn off regularly and is the SH reaction reduced to a level that is characterized by a nominal burn with pressure and thrust built-up, but without a strong global reaction and fragmentation of the case?

In that first phase of mitigation studies, the igniter was triggered manually when the oven reached the onset temperature of the exothermal reaction of the HBR propellant. The behaviour of the HBR propellant at soak-temperatures beyond 100°C and, in particular, the burn rates at such high temperature levels were investigated by small-scale 2-inch rocket motor tests. Those small-scale tests showed, that the burn-rate/pressure relation remained regular and on top of the nominal constant "Klemmungs"-line - even in the high temperature regime! That result also led to the successful design and qualification of the high temperature igniter using test firings in heated bombs.

Figure 9 shows the head-end pressure and the thrust measured during the SH test with mitigation. After ignition at $\gg 100^\circ\text{C}$ soak temperature, the pressure reached a level 220 bar. Unfortunately, the thrust measurement was truncated due to a wrong switch setting in the thrust-signal amplifier. However, internal ballistics calculations together with the measured high-temperature 2-inch burn-rate data gave an estimate of the maximum thrust to be 80 kN to 100 kN. The latter is approximately twice the nominal thrust of the motor. As the data indicate, the dummy nozzle did not withstand the heat/pressure load and was ejected. The motor burned off regularly and the CFC case with a nominal (i.e., room temperature) burst pressure above 300 bar remained undamaged. Therefore, the results of the SH-mitigation test indicated that an early ignition device can mitigate the severe and global SH reaction and reduce it to a comparatively controlled rocket-motor burn with a directional (vs. global) reaction, i.e., with formation of thrust, without fragmentation of the case.

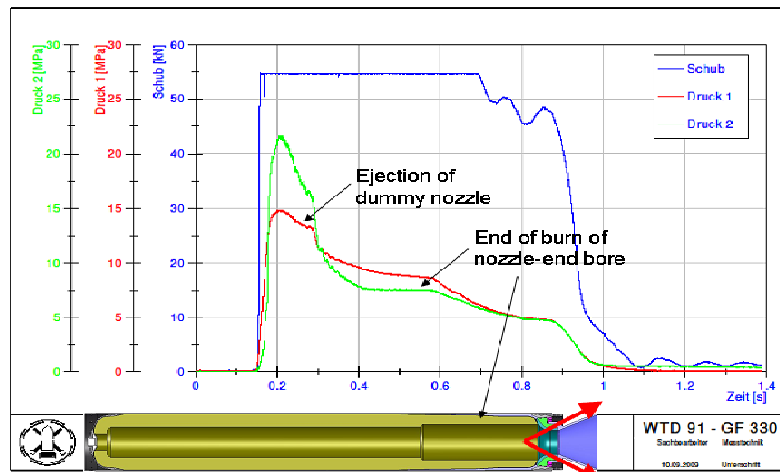


Figure 9: SH mitigation by early ignition, pressure and thrust evolution.

4. IM Simulation

Since SH tests cause the most severe reaction levels and also require the most effort of all STANAG IM-tests, numerical modelling focused on the physics and understanding of SH case. Using data from small-scale DSC calorimetry tests (measured by Dr. Koch, WTD91 310, Meppen) a reaction kinetics model was implemented in a Finite Element (FE) program. The heat release in the FE-volume is caused by the exothermal reaction of the propellant and depends on the local temperature and the reactive material left in the finite volume.

Figure 10 shows a typical result of a constant heating-rate DSC calorimeter test with the measured heat release as function of the oven temperature. The green area in the diagram marks the release of a small amount of heat that happens much earlier than the major reaction (i.e. the final burn of the sample). The early release of heat indicates the start of exothermal reactions and leads to the fact that, in the final stage of a SH test, the entire propellant grain will heat up exponentially and react almost simultaneously in its bulk state! Fig.10 also shows the FE-model of the HBR motor which includes the air-volume in the bore.

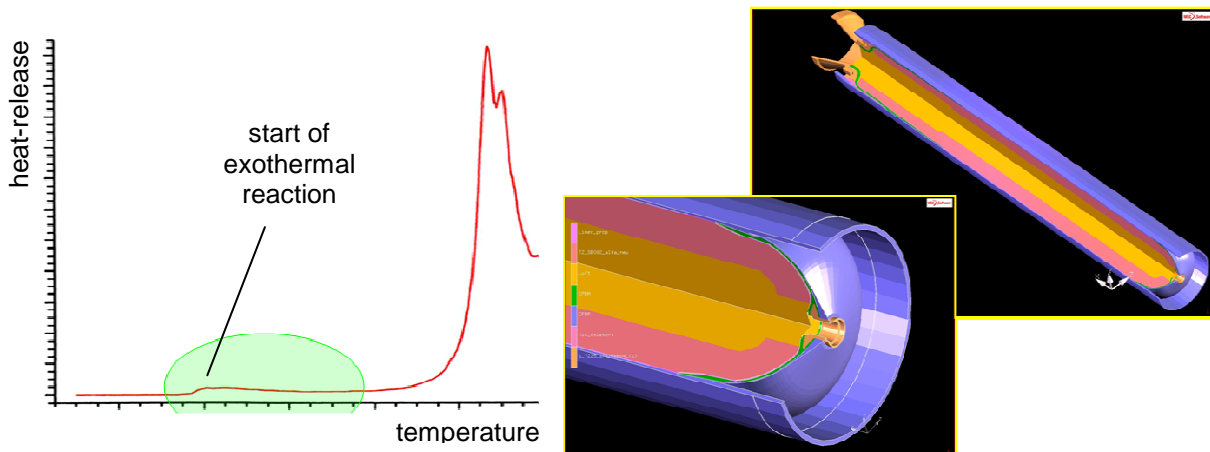


Figure 10: Results of DSC calorimetry and FE-model of the HBR motor.

Figure 11 shows the computed temperature distribution in the HBR rocket-motor and the air in the bore just before the SH-reaction. The computation is two-dimensional and used a measured 3.3°C/h oven-temperature profile as boundary condition. The results indicate the formation of a hot spot in the dome region close to the bore surface. At that location, the SH-reaction would actually start. While the temperature of the hot-spot is only 10K higher than that of the hot region in the rear of the motor, the residual part of the grain remains at oven-temperature level. The physical meaning of the hot-spot location is that this is the thermally best insulated region in the motor with the least amount of heat loss through conduction.

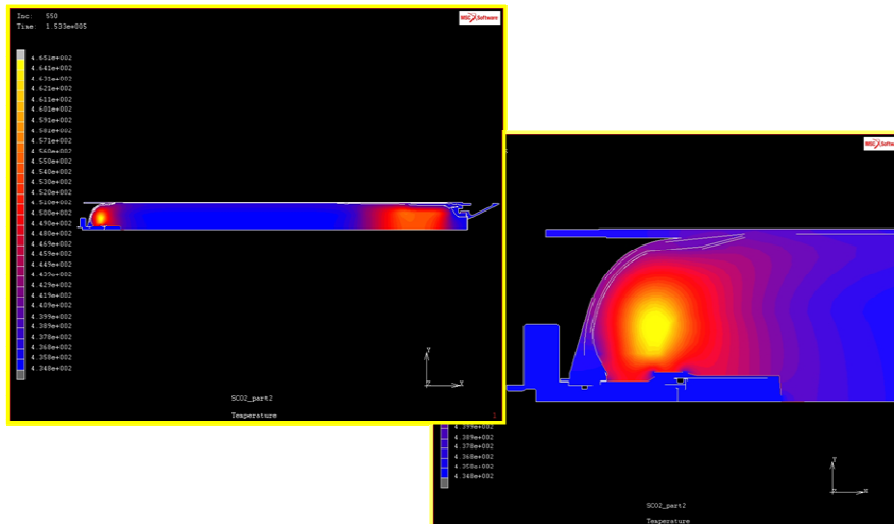


Figure 11: FE-temperature distribution of the HBR-motor just before the SH-reaction

Finally, Fig. 12 shows a comparison of computed and measured motor surface (T3) and bore-air (T_bore) temperatures. At both positions the agreement is better than 3K. Also, the evolution of the computed hot-spot temperature and its exponential rise towards the ignition temperature is shown. The computed reaction time (measured from the start of the 3.3°C/h gradient) is 120000 s or 33.3 h with a motor-surface temperature of T3 = 162°C. Those results compare very well to the measured 34.5 h reaction time at 162°C oven temperature.

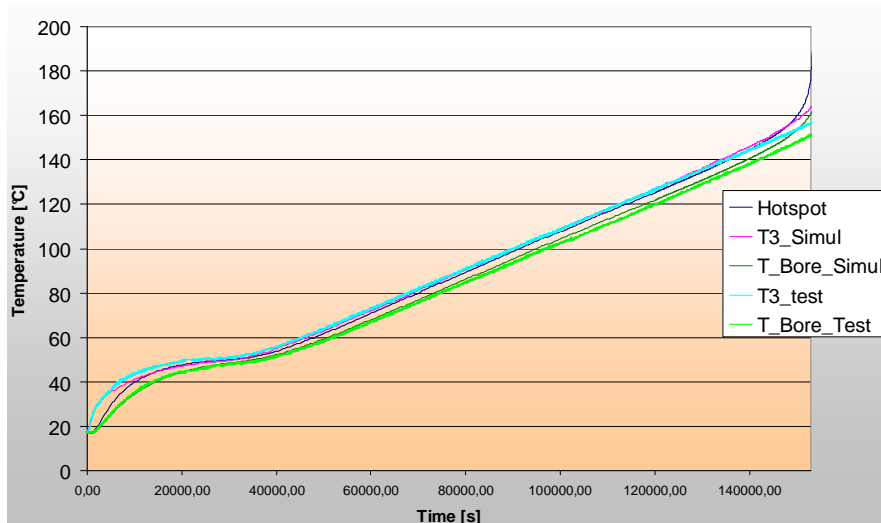


Figure 12: Computed and measured temperature evolution during the HBR SH test.

5. Summary and Outlook

The major results of the IM Technology Study were to improve the knowledge on the IM behaviour of solid propellant rocket motors by

1. extended large- and small-scale test campaigns at the WTD91 proving ground Meppen,
2. IM-simulations and implementation of new IM material models, and
3. design and test of promising mitigation elements for the Slow Heating case.

In the future, the focus of IM technology work will be on small-scale and high temperature testing in the area of burn rate characteristics, propellant reaction kinetics, and material properties. Also, the results of FH tests will be investigated further by looking at the boundary conditions and the characteristics of Kerosin and Propane gas fires. Finally, the simulation of dynamic (and, therefore, global) reactions that cause the fragmentation of the rocket motor will be intensified.